Digest Journal of Nanomaterials and Biostructures Vol. 11, No. 3, July - September 2016, p. 821 - 831

THE PHOTOCHROMIC PROPERTIES OF REDUCED GRAPHENE OXIDE DOPED TUNGSTEN/MOLYBDENUM TRIOXIDE NANO-COMPOSITES

L. SIKONG[abc*], P. CHOOPOOL[abc], K. KOOPTARNOND[abc]
[a]*Department of Mining and Materials Engineering, Faculty of Engineering,*
[b]*Center of Excellence in Nanotechnology for Energy (CENE), Faculty of Science,*
[c]*Center of Excellence in Materials Engineering (CEME), Faculty of Engineering,*
Prince of Songkla University, Hat Yai, Songkhla, 90112, Thailand

The reduced graphene oxide (RGO) doped tungsten trioxide/molybdenum trioxide (WO_3/MoO_3) composite powders were successfully prepared by simple co-precipitation method with the difference RGO concentrations. The effect RGO on crystal structure, optical properties, and the photochromic properties were investigated. The synthesized composite powders having the mixed phase between *h*-WO_3 and amorphous, high defect concentration and band gap energy varying from 2.83 eV to 3.15 eV depended on the mixture composition can be stimulated by UV or visible light and change the color from white or light gray to deep blue. The composite film was prepared by casting synthesized powders that dispersed in polymer matrix and their photochromic properties under UV irradiation were studied by the color difference (ΔC) measured by means of colorimeter. The $1.3x10^{-3}$ wt% RGO-doped WO_3/MoO_3 composite films show good color change that can turn to dark blue after irradiation and can return to the original color about 94% within 10 min by heating at 80 °C. The films exhibit high stability of photochromic performance after repeated tests.

(Received May 18, 2016; Accepted August 6, 2016)

Keywords: Tungsten trioxide/molybdenum trioxide, Reduced graphene oxide, Photochromic properties, Co-precipitation method, UV light

1. Introduction

Transition metal oxides are important materials have the widely range of application in photocatalyst, energy storage, gas sensors and chromic materials including electrochromic and photochromic materials. Tungsten trioxide (WO_3) and molybdenum trioxide (MoO_3) are transition metal oxides and semiconductors that show the photochromic properties under UV light irradiation [1-6]. The coloration of WO_3 or MoO_3 is due to photo-generated electron-hole pair between adjacent particles leading to partial hydrogen bronze formation and status change valence of tungsten or molybdenum ion from W^{6+} (transparent) to W^{5+} (blue) ($W \rightarrow W$) or Mo^{6+} (transparent) to Mo^{5+} (blue) ($Mo \rightarrow Mo$) [7-10].

The way for improving the photochromic performance of WO_3 and MoO_3 is to develop the multicolor photochromic material with fast responsibility which depends on the structure, hexagonal, RO_3 (R is W or Mo) that contain the RO_6 octahedral arranged six membered ring sharing corner oxygen along (001) plane to form many open-tunnels, empty or fulfills with water molecules, easily for intercalation of ions (Li^+, H^+, K^+ and Na^+) different another ReO_3 stable phases [10,11]. These blue metastable phase WO_3 nanostructure after visible light irradiation was turned back to original color after annealing at 90 °C for 7 min [12]. The blur film of hexagonal phase WO_3 after UV light irradiation was turned back to original color after ~60 days in dark condition [13]. The mixed oxide, semiconductor such as MoO_3, TiO_2, ZnSe and CdS [3,14-18] and doped with metals such as Au [19] shown the best photochromic responsibility. The WO_3/MoO_3 film color turned blue under visible light that suggested the electron transfer between mixed metal

* Corresponding author: lek.s@psu.ac.th

oxide for coloration [20,21]. The metal, Zr doped WO_3 amorphous film show good photochromic properties under visible light [22]. The hybrid materials $CdS/TiO_2/WO_3$ semiconductors turned blue under visible light but electron was suppressed the recombination [1].

Reduced graphene oxide (RGO) is the advanced materials that structure with the monolayer of carbon atom packed into a 2D honeycomb lactic exhibited high photocatlytic performance because of its high electrical conductivity, excellent mobility of charge carriers (20,000 cm^2/Vs. at room temperature) and large specific surface area (2,630 m^2/g)[24]. The semiconductor doped with RGO shows high photocatalytic performance due to its excellent electron acceptor that can retard the recombination of the electron-hole pair and now are applied for the photocatalyst, gas sensors and energy conversion[13, 25, 26].

The aim of this work was to prepare RGO doped WO_3/MoO_3 composite materials by the simple co-precipitation method. The effect of RGO concentration on structure, morphology, and photochromic property of the composite materials was determined. The stability of photochromic composite film was also observed.

2. Materials and Methods

2.1 Synthesis of Graphene Oxide (GO)

GO was fabricated by using the modified Hummer's method [27]. One gram of natural graphite flake (-10 mesh, 99.9%, Alfa Aesar), 0.5 g of $NaNO_3$ (Ajax Finechem) and 23 ml of sulfuric acid (98%, J.T. Baker) were mixed and stirred in ice bath for 30 min. Three grams of potassium permanganate ($KMnO_4$, Ajax Finechem) was slowly added to the stirred suspension and kept the temperature below 20 °C for 30 min then the solution was continually stirred at 35 °C for 24 h, the dispersion turned to brownish-gray paste. After that, 40 ml of distilled water was added to the mixture then the temperature reached $>$90 °C, further stirred for 30 min. After cooled, added with 10 ml of H_2O_2 and 140 ml of distilled water, stirred again for 15 min. The product was filtered, washed with water, 1M HCl and ethanol. Finally, GO powder was collected and dried at 80 °C for 24 h.

2.2 Reduction of GO

GO was reduced by the chemical reduction method [28-30]. The 0.5 g of GO and 100 ml of 0.5% NH_4OH (37%, J.T. Baker) were mixed and stirred at 60 °C for 30 min until the dispersion turned yellow-brown, then 4 mM ascorbic acid (99.5%, Poch) was mixed and kept at 95 °C for 60 min. The mixture was filtered and washed with distilled water and ethanol until pH $\sim$6 then the product was collected and mixed with 100 ml of distilled water for making 5 mg/ml RGO dispersion.

2.3 Preparation of RGO-doped WO_3 and RGO-doped WO_3/MoO_3 Powders by Co-precipitation Method

WO_3 powders (99.5%, Sigma-Aldrich) were dissolved in 100 ml of 2.5% NH_4OH at 60 °C for 30 min to prepare WO_3 (W) solution. After stirred for 15 min, the RGO dispersion with varying concentrations of 0.02 and 0.04 mg/ml (or 1.3×10^{-3} and 2.6×10^{-3} wt%) was added into the solution to make the W2 and W4 samples, respectively. The mixture was held at 85 °C while 30 ml HNO_3 (70%, J.T. Baker) was slowly added and stirred for 60 min. As the reaction proceeded, the mixture turned to greenish-yellow precipitates. Finally, the precipitates were filtered, washed with water and dried at 50 °C for 24 h. Then the RGO-doped WO_3 powders were collected and kept in dark condition. For RGO-doped WO_3/MoO_3 powders preparation, WO_3 powders were dissolved in 100 ml of 2.5% NH_4OH at 60 °C for 30 min and mixed with ammonium heptamolybdate tetrahydrate ($(NH_4)_6Mo_7O_{24}$ .4 H_2O, Ajax Finechem) to prepare WO_3/MoO_3 (WM) solution with the 50 wt% WO_3/MoO_3. After stirred for 15 min, the RGO dispersion with varying concentrations of 0.65×10^{-3}, 1.30×10^{-3}, 2.0×10^{-3} and 2.6×10^{-3} wt% was added into the solution to make the WM1, WM2, WM3 and WM4 samples, respectively. Afterward, 30 ml HNO_3 was slowly dropped into the solution and stirred at 85 °C for 60 min, the product was filtered,

washed, dried at 50 °C for 24 h. Finally, RGO-doped WO_3/MoO_3 powders were collected and kept in dark condition.

2.4 Fabrication of Composite Films

The 0.4 g polyvinyl chloride powders (PVC, MW = 2,000-3,000) were dissolved in 10 ml N, N-Dimethylformamide (DMF, 99.5%, Ajax Finechem) at 60 °C for 30 min. After that, the 0.4 g W or WM or WRGO or WMRGO powders were dispersed into the clear solution and sonicated for 30 min. The mixture was cast onto the petri dish at 80 °C and dried it for 3 h. Finally, the composite films were collected and kept in dark condition.

2.5 Materials Characterization

The microstructure of composite powders were analyzed using X-ray diffraction (XRD) (X'Pert MPD, Philips CuKα (λ = 1.5405Å) radiation). The Raman spectra were taken by T64000 triple monochromator Raman spectroscopy, Jobin Yvon Horiba, France using 150 mW of the 532 nm solid state lasers exciting. UV-vis absorption spectra were obtained by UV-2401, Shimadzu UV-vis spectrophotometer. Scanning electron microscopy (SEM) was performed on FEI Quanta 400 at accelerating voltage of 25 kV and Energy-dispersive x-ray measurements (EDX), Oxford. Transmission electron microscopy (TEM) was carried out with JEOL 2010 microscopy with the acceleration voltage of 200 kV.

2.6 Photochromic Properties Test

The photochromic property of as-prepared composite films was investigated by a color difference meter (HP-200 Precise Color Reader). The color standard according to the CIE Lab uniform color was used to determine the optical property of the samples after treated under UV irradiation with lamps of 60 watts power, for 50 min. The color differences were calculated to compare color before and after photo-treated. After measured the color, the photo-treated film was heated in an oven at 80 °C for designated times in the range of 0 to 50 min in order to bleach the film color to be an original color. The color changing was measured during bleaching for designated time. The color difference was calculated by formula below:

$$\Delta C = \left[(\Delta L^*)^2 + (\Delta a^*)^2 + (\Delta b^*)^2\right]^{1/2} \quad (1)$$

where ΔC is the color difference of powder before and after being irradiated. L^* stands for the transparency index while a^* and b^* refer to the chroma indexes[31].

3. Results and Discussion

3.1 XRD Analysis

To study the structure of all samples, the XRD patterns of samples prepared at various concentrations of RGO were analyzed and given in Fig. 1**.** The pure W, W2 and W4 were identified as tungsten oxide monohydrate ($WO_3.H_2O$), having the orthorhombic structure (o-WO_3) at the main peak 2θ = 16.5, 25.6, 34.1 and 34.9 degrees from Fig. 1(b) [32] while the WM samples presented pure amorphous phase. For RGO doping samples (WM1-WM4), they displayed the crystallinity of mixed phase that hexagonal phase WO_3 (h-WO_3) showed at the peak 2θ = 14.0, 23.2, 24.28, 27.0, 28.1, 33.8 and 53.5 degrees and an o-WO_3 [4, 14]. The proportion of h-WO_3 in WM2 sample was about 75% and it increased with increasing RGO ratio in the samples. For pure RGO, the main peak showed at 2θ = 25.4 degrees (Fig. 1(b))**.** The crystallite size (d) of composite powder was estimated from Scherrer' equation [10],

$$d = 0.9\,\lambda / \beta \cos\theta \quad (2)$$

where d is the crystallite size, θ is the Bragg angle, λ is the x-ray wavelength CuKα (λ= 1.5405Å) and β is the full width at a half maximum of the diffraction peak (FWHM).

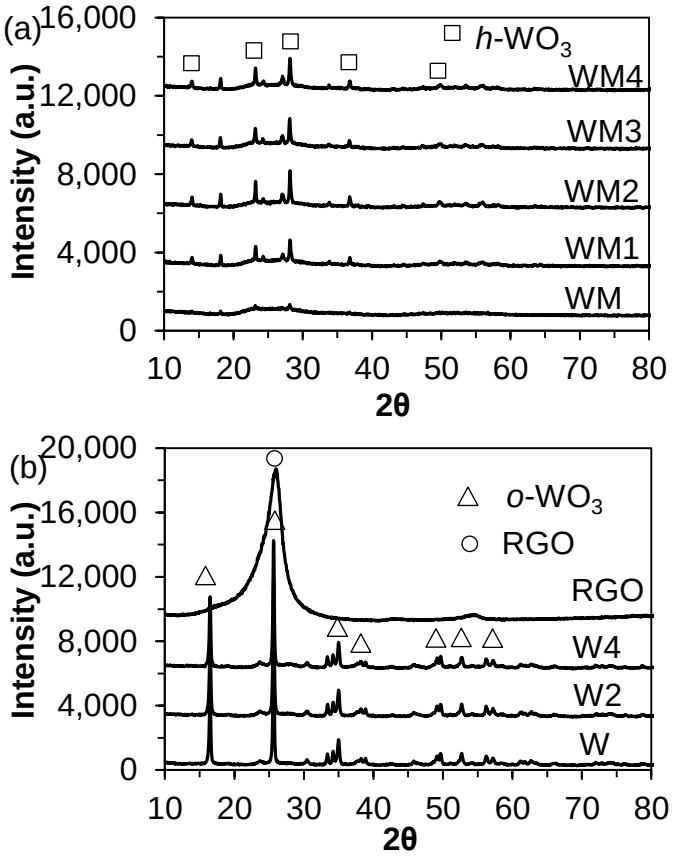

Fig. 1. XRD patterns of (a) WO_3/MoO_3 doped with RGO and (b)WO_3 doped with RGO

The crystallite sizes analyzed from XRD peak using the Scherrer' equation from Eq.(2), show at Table1**.** The crystallite sizes of all samples were about 41 nm except for that of WM4 sample it was 55 nm due to the growth of h-WO_3. It was noted that RGO doping had an effect on promotion of h-WO_3 of WO_3/MoO_3 composite which led to the enhancement of their photochromic property.

3.2 The Morphologies Analysis

The morphologies of composite powders were investigated by SEM and TEM. The SEM images of powders at various RGO concentrations are shown in Fig. 2(a-d). All of the samples displayed the irregular rounded shape of agglomerated powders having particle size determined by TEM image in Fig. 2(e) for WM2 around 50-100 nm**.** The W, O, M and C elements were found in WM2 sample analyzed by using X-ray mapping of EDX technique (Fig. 2(f)).

3.3 The Optical Properties

The UV-vis absorbance spectra of the synthesized WO_3 and RGO doped WO_3 powders illustrated in Fig. 3(a) exhibit strong absorption wavelength at lower than 525 nm while those of WO_3/MoO_3 and RGO doped WO_3/MoO_3 samples decrease with increasing RGO concentration and the strong absorption wavelength is at below 470 nm. It is indicated that the samples can be activated by UV light to visible light.

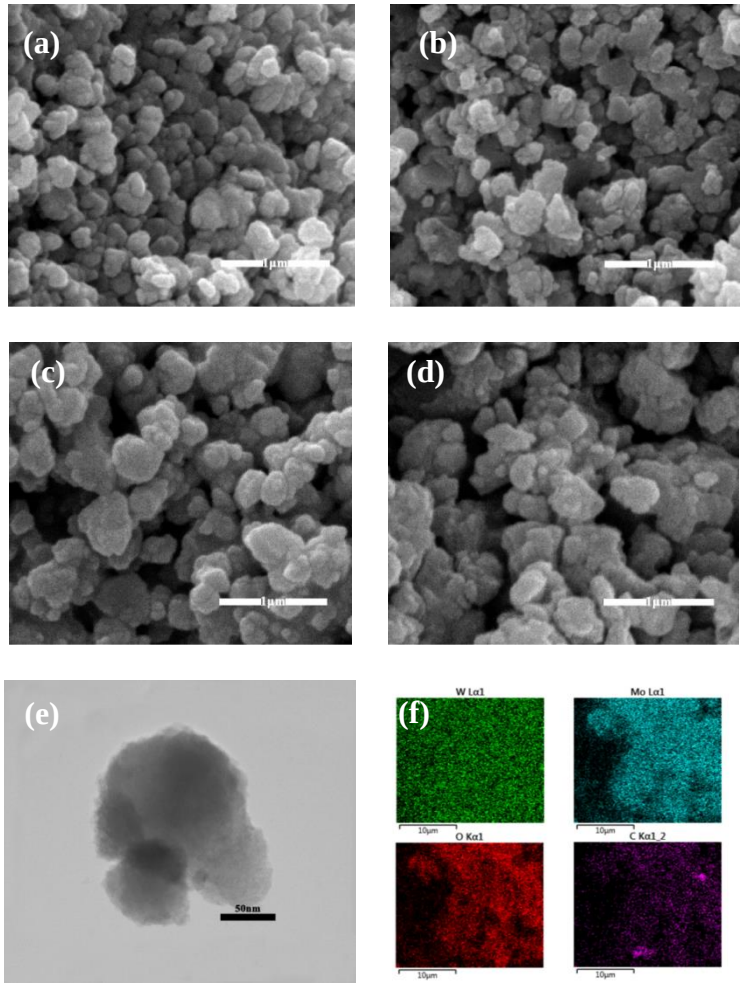

Fig. 2. SEM images of (a) W, (b)WM, (c)WM2, (d)WM4, (e) TEM image and (f) EDX pattern of WM2 sample

The direct band gap of all powder was calculated from the relationship below:[10, 33]

$$\alpha E = A'(E - E_g)^m \tag{3}$$

where E_g, A', E are the direct band gap, a constant and the photon energy ($E = hc/\lambda$), respectively. m = 1/2 for direct band gap and m = 2 for indirect band gap. The absorption coefficient (α) was estimated by

$$\alpha = A/d' \tag{4}$$

where A is the measured absorbance and d' is the thickness of samples in UV-vis cell (0.4 cm) and E was approximated by

$$E = 1240/\lambda \tag{5}$$

where λ is the measured wavelength in nm.

The direct band gap of all product was estimated by extrapolation of the linear portion of $(\alpha h\nu)^2$ as a function of E to $\alpha E = 0$ (where $E = E_g$), as shown in Fig. 3 (b) and Table 1. The band

gap energy of WO_3 was increased when mixed with MoO_3 as a composite by increasing from 2.83 eV in WO_3 to 2.95 eV in WO_3/MoO_3 due to the *o*-WO_3 changing to an amorphous phase. RGO has no effect on the increasing band gap energies of WO_3 but it has such effect for WO_3/MoO_3 composite. The E_g of WM1 was 3.15 eV while those of WM2, WM4, and WM3 were 3.10, 3.10 and 3.05 eV, respectively. It is due to the change in their microstructure from an amorphous to hexagonal phase resulted from RGO doping in the WO_3/MoO_3 composite.

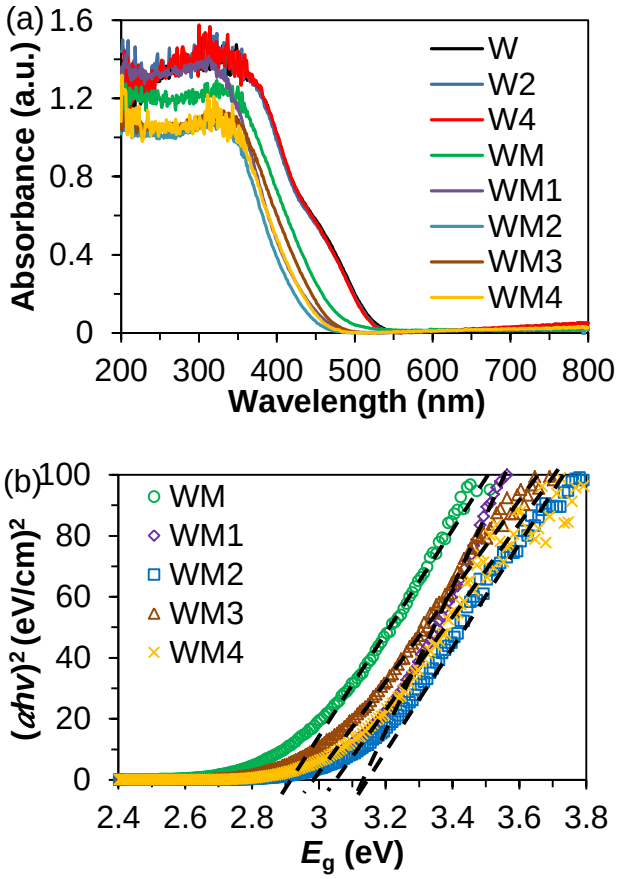

Fig. 3. UV- vis absorbance spectra (a) and plot of $(\alpha h\nu)^2$ as a function of E for the RGO-doped WO_3/MoO_3 composite powders (b)

The defect concentration or oxygen vacancies concentration were estimated from formula below[10],

$$\alpha E = \alpha_0 \exp(E / E_0) \tag{6}$$

where α is the absorption coefficient calculated from absorbance, α_0 is a constant, E is the photon energy and E_0 is an empirical parameter that depending on defect concentration, temperature and structure disorder.

The defect concentration (E_0) of the synthesized composites was estimated by the slope that a plot of $ln(\alpha)$ as a function of E from Eq.(6) shown in Table 1. The defect concentration of WO_3/MoO_3 was higher than that of WO_3 due to the presence of an amorphous phase in WM sample. RGO doping has an effect on enhancement of defect concentration of RGO-doped WO_3 and RGO-doped WO_3/MoO_3. The near optimal concentration of defect or oxygen vacancies concentration was found in WM2 composite. The increase in defect concentration depends on the sample crystallinity when RGO in the composite increased, it leads to the increasing hexagonal phase and defect in the crystal. Their defects are important factors affecting the photochromic properties[5]. The lower crystalline quality of WO_3/MoO_3 and RGO-doped WO_3/MoO_3 shows a

large amount of defects or oxygen vacancies those act as the color centers and recombination centers between conduction band (CB) electrons and valence band (VB) holes in the metastable *h*-WO_3 phase. The high defect concentration contains water molecules for promoting the photon insertion and the active electrons transferring between adjacent molecules.

Table 1. Crystallite size, band gap energies and defect concentration (E_0) of the samples synthesized with varying RGO

Sample	RGO (wt%)	Sample acronym	Crystallite size (nm)	Band gap energy (eV)	Defect concentration (E_0)
WO_3	-	W	41.4	2.83	1.68
	1.3×10^{-3}	W2	41.4	2.85	1.90
	2.6×10^{-3}	W4	41.4	2.85	1.77
WO_3/ MoO_3	-	WM	Amorphous	2.95	2.35
	0.65×10^{-3}	WM1	41.6	3.15	2.25
	1.3×10^{-3}	WM2	41.6	3.10	2.43
	2.0×10^{-3}	WM3	41.6	3.05	2.19
	2.6×10^{-3}	WM4	55.5	3.10	2.10

3.4 Photochromic Properties

The photochromic properties of films are shown in Fig. 4(a). The coloration and bleaching processes were studied by using the color difference ΔC of film before and after irradiation with UV light for 50 min, calculated from Eq.(1)**.** The ΔC of films decreased with increasing amount RGO becuase RGO changed the film's color to darkened color, therefore ΔC before and after irradiation were less than the undoped RGO film where WM exhibited the greatest ΔC that changed from white to dark blue after 50 min under UV irradiation. However, the lower ΔC of WO_3 and RGO-doped WO_3 than other films indicated that the *o*-WO_3 has poor photochromic property. After thermal treated in oven at 80 °C, the bleaching process (blue color of the composite film returning to original color) determined from ΔC, was observed for changing color (Fig. 4 (a)). WO_3/MoO_3 and 1.3×10^{-3} wt% RGO doped in WO_3/MoO_3 (WM2) films showed high reversibility of 93-94 % within 10-20 min heating time but the bleaching rate of RGO-doped WO_3 film was found to be very slow only 5 % reversibility of W2 (WO_3 doped with 1.3×10^{-3} wt% RGO) was observed after 5 hour-heating.

The high photochromic performance of WM and WM2 composite is due to the disordered crystals with a large amount of oxygen vacancies resulted from their mixed phase (amorphous and hexagonal) containing more water molecules, leading to a high electron mobility and a high photon insertion [7, 8]. The stability of photochromic property of WM2 film was investigated for 5 cyclic photochromic tests including 20 min-UV irradiation and 20 min-thermal treatment at 80 °C illustrated in Fig. 4(b). It was found that the ΔC of the fifth cycle can be returned to original color 85 % within 20 min-thermal treatment at 80 °C.

Fig.5 shows the color photograph of films that exposed to UV light 50 min and thermal treated at 80 °C for 20 and 360 min. Under UV irradiation, the WO_3/MoO_3 film changed its colors from white to dark blue while the RGO-doped WO_3/MoO_3 films changed their colors from gray to dark blue. The WO_3 and RGO-doped WO_3 having pure orthorhombic phase changed color from yellow to dark yellow[14, 31, 34]. Afterward, the samples were kept in an oven at 80 °C, WO_3/MoO_3 and RGO-doped WO_3/MoO_3 films can return to the original gray color but WO_3 and RGO-doped WO_3 films cannot return to the original yellow color.

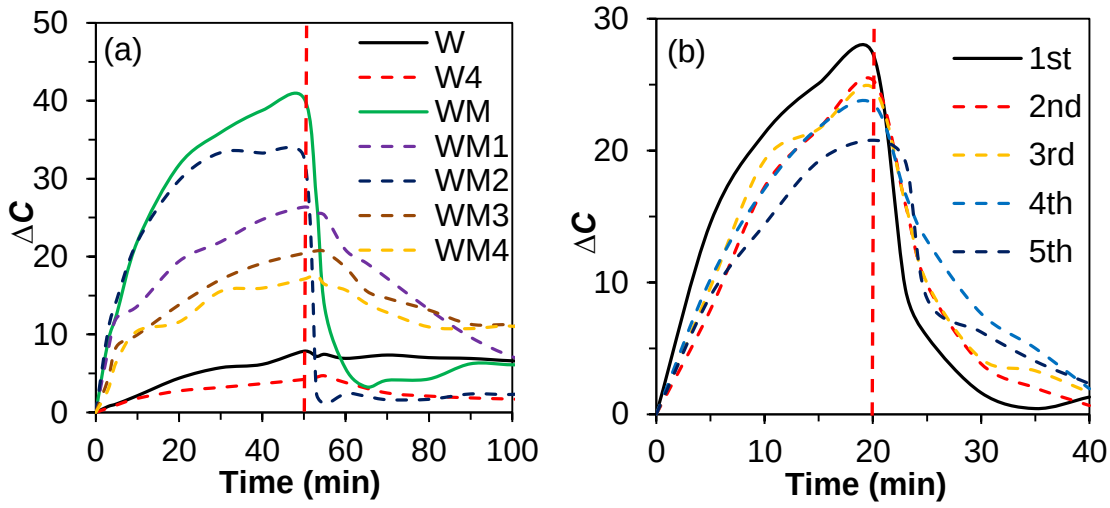

Fig. 4. The color difference (ΔC) of (a) RGO-doped WO_3 and WO_3/MoO_3 composites irradiated under UV light for 50 min and then thermal treated in an oven at 80 °C for a designated time and (b) the stability of photochromic property of WM2 film treated for 5 cycles

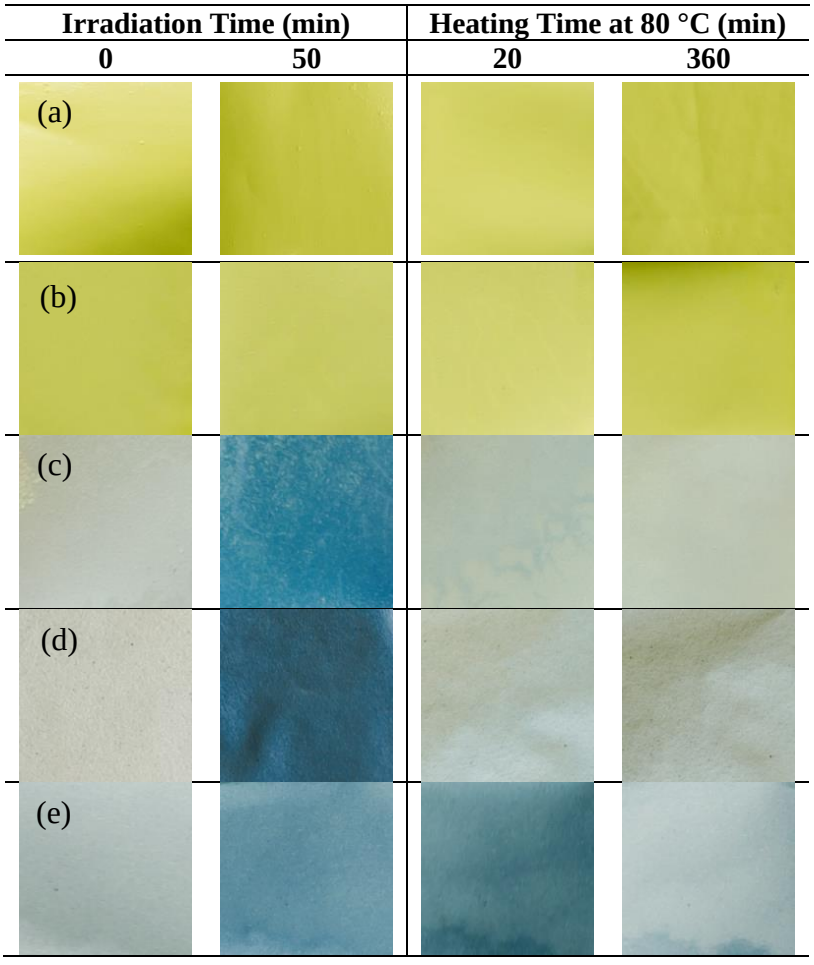

Fig. 5. The photographic images of samples: (a)W, (b)W4, (c)WM, (d)WM2 and (e) WM4 irradiated under UV light for 50 min and then kept in oven at 80 °C f or 20 and 360 min

From literature review explained this phenomena in two models photochromic mechanism of WO_3 and MoO_3 under UV light irradiation that light energies higher than band gap energies where the electron in the valence band (VB) take enough energy and jump to the conduction band (CB), leaving positive charge holes in the VB. 1) Some activated electron and hole were reacted with water molecules to produce oxygen (O_2) and photon (H^+) then the film turned blue due to photon absorption of particles to form hydrogen bronze ($H_xR_x^{5+}R_{1-x}^{6+}O_3$). In addition, the photo-generated electron-hole recombination occurred. 2) The excited electron could move by diffusion on surface and transfer to adjacent particles that valence electron of acceptor particles changed from 6+ to 5+ and color turned blue[7, 8]. The coloration mechanism of the sample supported by Raman spectra of WM2 sample before and after UV irradiation is shown in Fig. 6**.** The spectrum before irradiation creates the peak at 350 cm^{-1} (a), 700 and 800 cm^{-1} as due to vibration of the $W^{6+}-O$, the peak 450 cm^{-1} (b) and 950 cm^{-1} for $W^{6+}=O$ bonds. After irradiation, was found the vibration and low intensities at main peak from the $W^{5+}-O$ and $W^{5+}=O$ bonds, hydrogen atom inserted in WO_{3-y} structure what forming weaker bond, lower energies than $W^{6+}-O$ and $W^{6+}=O$ and the electron reduce from W^{6+} to W^{5+} ion so the color was changed to dark blue and the intensities of peak were reduced [35].

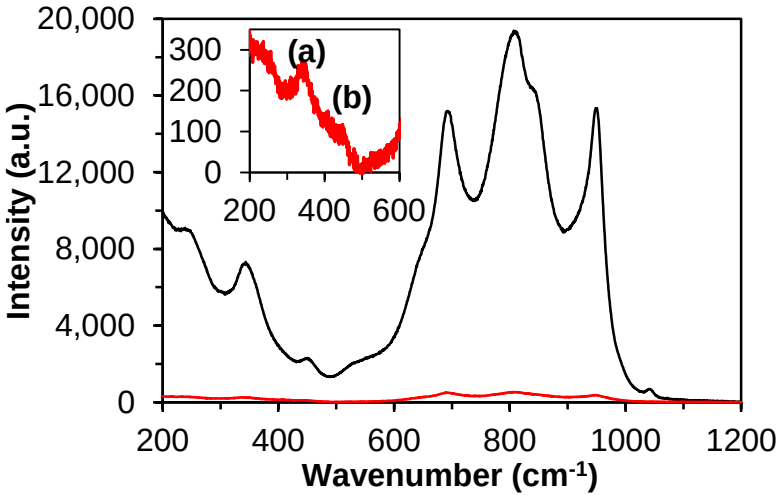

Fig. 6. The Raman Spectra of WM2 before (black line), after UV irradiation 48 h (red line) and the peak after irradiation focused at the wavenumber of 200 – 600 cm^{-1}(inserted graph)

The WO_3/MoO_3 composite materials exhibited the enhanced photochromic performance than pure WO_3 or MoO_3 because in mixed oxide composite materials, electrons transfer from Mo^{5+} to W^{6+} (Mo → W), assumed that MoO_3 work function was higher than WO_3[7, 8, 21, 36]. The improvement of the reversibility of the photochromic properties [37] is due to RGO having a charge – carrier mobility of 20,000 cm^2/Vs, resulted in an increase in charge separation efficiency. Under UV light irradiation, RGO with 2D conjugated $\pi-\pi$ graphitic carbon network, great electrical conductivity and the good electron acceptor, it could efficiently transfer photo-generated electron away from one to adjacent particles[24-26, 38]. Therefore, during irradiation, the photo-generated electrons were continuously transferred through RGO from CB of WO_3 to CB of MoO_3 and hole from VB of MoO_3 to VB of WO_3 that electrons were trapped at CB of MoO_3 and holes were trapped on VB of WO_3, both of these were migrated by electron reduced water to H^+ and holes oxidized water to O_2, forming the hydrogen bronze (turned blue). In heating condition, electrons from CB of MoO_3 were excited and transferred to holes in VB of WO_3 for recombination and color bleaching process[39].

4. Conclusion

RGO-doped WO_3/MoO_3 composite materials were successfully fabricated by the simple method, co-precipitation at varying concentrations of RGO. The composite microstructure was a mixed phase (~75% *h*-WO_3 and ~25% amorphous) which *h*-WO_3 increased with increasing RGO concentration. The RGO-doped WO_3/MoO_3 composite powders having the irregular rounded shape of agglomerated fine particles with size about 50-100 nm, a large amount of defects and band gap energy of 3.10 eV were dispersed in PVC matrix solution to form the composite films for photochromic testing under UV irradiation for 50 min. For RGO-doped WO_3/MoO_3 films, their colors changed from gray to dark blue while for WO_3/MoO_3 film, it changed from white to deep blue. The WM2 (1.3×10^{-3} wt% RGO-doped WO_3/MoO_3) film exhibited the best coloration with 94% reversibility by 10 min-heating at 80 °C and it had fast photochromic response and stability.

Acknowledgments

Financial supported from Center of Excellence in Nanotechnology for Energy (CENE), Prince of Songkla University is acknowledged. The authors are thankful to the Department of Chemistry, Faculty of Science for the use of UV-vis Spectrophotometer. The authors also wish to acknowledge the Center of Excellence in Materials Engineering (CEME) and Department of Mining and Materials Engineering, Faculty of Engineering and The Graduated School, Prince of Songkla University.

References

[1] H-i. Kim, J. Kim, W. Kim, W. Choi, J Phys Chem C **115**, 9797(2011).
[2] J.G. Zhang, D.K. Benson, C.E. Tracy, S.K. Deb, A. Czanderna, C. Bechinger, J Electrochem Soc **144**, 2022(1997).
[3] J. Scarminio, A. Lourenço, A. Gorenstein, Thin Solid Films **302**, 66(1997).
[4] R. Huang, Y. Shen, L. Zhao, M. Yan, Adv Powder Technol **23**, 211(2012).
[5] S.K. Deb, Proc R Soc A **304**, 211(1968).
[6] H. Miyazaki, Y. Baba, M. Inada, A. Nose, H. Suzuki, T. Ota, Bull Chem Soc Jpn **84**, 1390(2011).
[7] A.I. Gavrilyuk, Electrochim Acta **44,** 027(1999).
[8] T. He, J. Yao, J Photochem Photobiol C **4,** 125(2003).
[9] H Zheng, J.Z. Ou, M.S. Strano, R.B. Kaner, A. Mitchell, K. Kalantar-zadeh, Adv Funct Mater **21**, 2175(2011).
[10] P. Jittiarporn, L. Sikong, K. Kooptarnond, W. Taweepreda, Ceram Int **40**, 13487(2014).
[11] W. Sun, M.T. Yeung, A.T. Lech, C.W. Lin, C. Lee, T. Li, X. Duan, J. Zhou, R.B. Kaner, Nano letters **15**, 4834(2015).
[12] R.J.D. Tilley, Int J Refract Met Hard Mater **13**, 93(1995).
[13] N. Li, Y. Zhao, Y. Wang, Y. Lu, Y. Song, Z. Huang, Y. Li, J. Zhao, Eur J Inorg Chem 2015, 2804 (2015).
[14] S. Songara, V. Gupta, P.M. Kumar, J. Singh, L. Saini, G.G. Siddaramana, V.S. Raj, N. Kumar, J Phys Chem Solids **73**, 851(2012).
[15] D. Sánchez-Martínez, A. Martínez-de la Cruz, E. López-Cuéllar, Mater Res Bull **48**, 691(2013).
[16] K. Gesheva, A. Szekeres, T. Ivanova, Sol Energy Mater Sol Cells **76**, 563(2003).
[17] S.A. Tomás, M.A. Arvizu, O. Zelaya-Angel, P. Rodríguez, Thin Solid Films **518**, 1332(2009).
[18] S. Higashimoto, N. Kitahata, K. Mori, M. Azuma, Catal Lett **101,** 49(2005).
[19] S. Yamazaki, T. Yamate, K. Adachi, Colloids Surf A Physicochem Eng Asp **392**, 163(2011).

[20] T. He, Y. Ma, Y. Cao, Y. Yin, W. Yang, J. Yao, Appl Surf Sci 180, 336(2001).
[21] T. He, J. Yao, Prog Mater Sci **51**, 810(2006).
[22] H.M.F. Ahmed, N.S. Begum, Bull Mater Sci 36, 45(2013).
[23] C. Avellaneda, Solid State Ionics **165**, 117 (2003).
[24] G. Zhao, T. Wen, C. Chen, X. Wang, RSC Adv **2**, 9286(2012).
[25] G. Williams, B. Seger, P.V. Kamat, ACS nano **2**, 1487(2008).
[26] Z. Gao, J. Liu, F. Xu, D. Wu, Z Wu, K. Jiang, Solid State Sci **14**, 276(2012).
[27] D.C. Marcano, D.V. Kosynkin, J.M. Berlin, A. Sinitskii, Z. Sun, A. Slesarev, L.B. Alemany, W. Lu, J.M. Tour, ACS nano **4**, 4806(2010).
[28] C.K. Chua, M. Pumera, Chem Soc Rev **43**, 291(2014).
[29] M.J. Fernández-Merino, L. Guardia, J.I. Paredes, S. Villar-Rodil, P. Solís-Fernández, A. Martínez-Alonso, J.M.D. Tascón, J Phys Chem C **114**, 6426(2010).
[30] X. Zhu, Q. Liu, X. Zhu, C. Li, M. Xu, Y. Liang, Int J Electrochem Sci **7,** 5172(2012).
[31] Y. Shen, D. Ding, Y. Yang, Z. Li, L. Zhao, Mater Res Bull **48**, 2317 (2013).
[32] S. Supothina, P. Seeharaj, S. Yoriya, M. Sriyudthsak, Ceram Int **33**, 931(2007).
[33] D. Souri, K. Shomalian, J Non-Cryst Solids **355**, 1597(2009).
[34] H. Zheng, J.Z. Ou, M.S. Strano, R.B. Kaner, A. Mitchell, K. Kalantar-zadeh, Adv Funct Mater **21**, 2175(2011).
[35] S.H. Lee, H.M. Cheong, J-G. Zhang, A. Mascarenhas, D.K. Benson, S.K. Deb, Appl Phys Lett **74**, 242(1999).
[36] J. Meyer, S. Hamwi, M. Kroger, W. Kowalsky, T. Riedl, A. Kahn, Adv Mater **24**, 5408(2012).
[37] J. Guo, Y. Li, S. Zhu, Z. Chen, Q. Liu, D. Zhang, W.J. Moon, D.M. Song, RSC Adv **2**, 1356(2012).
[38] Q. Xiang, J. Yu, M. Jaroniec, Chem Soc Rev **41**, 782(2012).
[39] A. Iwase, Y.H. Ng, Y. Ishiguro, A. Kudo, R. Amal, J Am Chem Soc **133**, 11054(2011).